Simulated LWA-1 Pulsar Observations

Bryan A. Jacoby[1], Wendy M. Lane[2], and T. Joseph W. Lazio[3]

September 27, 2007

Abstract

We present a preliminary analysis of the potential for pulsar observations with LWA-1. We estimate that of order 80 pulsars will be detectable in 1000 s with 16 MHz bandwidth at a center sky frequency of 72 MHz, with fewer pulsars detectable with decreasing frequency or bandwidth. We note that the chief difficulty in our estimates is the large uncertainty in the expected flux density at LWA frequencies calculated from flux densities and spectral indices measured at sub-meter wavelengths.

1 Introduction

The Long Wavelength Array (LWA) will have unprecedented sensitivity at frequencies below approximately 80 MHz. Radio pulsars have steep radio spectra and are potentially observable with the LWA, but the emission properties of pulsars at frequencies below about 100 MHz are largely unknown. We have estimated the number of pulsars that will be observable with the first phase of the LWA, LWA-1, using standard phase-synchronous pulse folding techniques. Here, we describe out methodology and results.

2 Methodology

We have simulated LWA-1 observations of pulsars in the ATNF Pulsar Catalogue[4]. We calculated the expected rms flux density, σ_S, of each observation using a modified form of the radiometer equation (units are given in square brackets),

$$\sigma_{S[\mathrm{Jy}]} = \frac{T_{\mathrm{sky[K]}}}{\sin\theta_{\max}\ G_{[\mathrm{K/Jy}]}\left(2\,\Delta\nu_{[\mathrm{Hz}]}\,t_{\mathrm{int[s]}}\right)^{1/2}}\left(\frac{\delta}{1-\delta}\right)^{1/2}, \tag{1}$$

where $\theta_{\max}$ is the pulsar elevation angle at transit, G is the telescope gain at the zenith, $\Delta\nu$ is the observed bandwidth, t_{int} is the integration time, T_{sky} is the sky temperature, and δ is

[1]bryan.jacoby@gmail.com
[2]wendy.lane@nrl.navy.mil
[3]joseph.lazio@nrl.navy.mil
[4]http://www.atnf.csiro.au/research/pulsar/psrcat/

the effective fractional duty cycle of the pulsar signal. The signal-to-noise ratio (S/N) of the observation is then simply the expected pulsar flux density S divided by σ_S.

We now describe in more detail how some of these terms were calculated.

2.1 Gain, G

The gain at zenith for an array of 256 dipole antennas at a wavelength λ is given by,

$$G_{[\mathrm{K/Jy}]} = \frac{A_\mathrm{e}}{2\,k} \approx \frac{10^{-26}}{1.38 \times 10^{-23}} \frac{256\ \eta\ \lambda^2_{[\mathrm{m}]}}{2}, \tag{2}$$

where A_e is the effective area, the fractional constant term relates G in units of K/Jy to the wavelength in meters and Boltzmann's constant k, and $\eta = 0.13$ is the aperture efficiency of a $\lambda/2$ dipole (Kraus, 1988, p. 45). Because of the spacing of the LWA antennas, the effective area saturates at a frequency of 37.5 MHz ($\lambda = 8$ m), giving a maximum gain of $0.77\,\mathrm{K\,Jy^{-1}}$. Mutual coupling is not well understood and was not considered in our calculations. LWA antenna stands receive two orthogonal polarizations, giving rise to the factor of $2^{-1/2}$ in Equation (1).

2.2 Sky Temperature, T_sky

The sky temperature T_sky at the position of each pulsar was extrapolated from the Haslam et al. (1982) 408 MHz sky survey to the relevant observation frequency assuming a spectral index of -2.6. Note that there may be significant sky temperature variation within the LWA-1 synthesized beam; this was not taken into account in our simulation.

2.3 Effective Duty Cycle, δ

The observed light curve or pulse profile of a radio pulsar differs from the intrinsic pulse profile due to propagation effects and instrumental artifacts. δ is simply the effective pulse width divided by the pulse period. The effective pulse width is the quadrature sum of the following terms:

2.3.1 Intrinsic Pulse Width

The intrinsic width of each pulsar's profile was calculated based on the W50 parameter in the ATNF catalog. W50 is the width of the profile at 50% of its peak value. Because these values are derived from observations at sub-meter wavelengths and pulse duty cycles typically increase with decreasing frequency, we have taken twice the W50 value to be the intrinsic pulse width at the frequencies of interest.

2.3.2 Sampling Interval

This is simply the time interval between samples in the data acquisition system, taken to be 1 ms in this simulation.

2.3.3 Scattering Time, $\tau_{\rm s}$

The interstellar scattering timescale for an observing frequency of 1 GHz was obtained for each pulsar's position and dispersion measure (DM) from the NE2001 Galactic electron density model (Cordes & Lazio, 2002). The scattering time was scaled to the observing frequency ν by $\tau_{\rm s} = \tau_{\rm s,\ 1\,GHz}\,(\nu/1\,{\rm GHz})^{-4.4}$.

2.3.4 Dispersion Smearing Time, τ_{DM}

The interstellar medium disperses the pulsar signal, with higher frequencies arriving at the antennas before lower frequencies. Assuming an incoherent or post-detection dedispersion data acquisition system, the full bandwidth of the telescope is broken up into many channels to mitigate the effects of dispersion. The remaining dispersive smearing within an individual channel of bandwidth $\Delta\nu_{\rm ch}$ is approximated by,

$$\tau_{DM[\rm s]} \approx \frac{8300\ DM_{[\rm cm^{-3}\,pc]}\ \Delta\nu_{\rm ch[MHz]}}{\nu^3_{\rm [MHz]}}, \tag{3}$$

where values of the sky frequency ν and the channel bandwidth $\Delta\nu_{\rm ch}$ in MHz and the dispersion measure DM in units of $\rm cm^{-3}\,pc$ give τ_{DM} in seconds. This approximation holds for $\Delta\nu_{\rm ch} << \nu$.

2.3.5 Inverse Frequency Resolution

The maximum fluctuation frequency that can be measured in a channel of finite bandwidth is the inverse of that bandwidth. The optimum channel bandwidth was chosen for each pulsar's DM and each observing frequency to optimize the competing effects of inverse frequency resolution and dispersion smearing, with a minimum channel bandwidth of 100 Hz.

2.4 Flux Density, S

Estimating the flux density of pulsars at low frequencies is the most uncertain part of this simulation, as few measurements exist in the literature. Of the 1627 pulsars in our all-sky simulation sample, only 66 have flux density measurements at or below 102.5 MHz. Pulsars are known as steep spectrum objects, but the flux density typically peaks around 100 MHz and decreases toward lower frequencies. The flux density of each pulsar was estimated as follows:

If a low frequency flux density measurement existed in the literature, we extrapolated from that measurement to the frequency of interest using a spectral index of 1.4. If multiple measurements existed for a given pulsar, we preferentially used the measurements of Cohen et al. (2007) from the VLA Low-Frequency Sky Survey (VLSS) at 74 MHz (13 pulsars). If no VLSS measurement existed for a pulsar, we used the measurements of Izvekova et al. (1981) in the following order of preference: 85 MHz (20 pulsars), 61 MHz (2 pulsars), and 102.5 MHz (31 pulsars).

If no low frequency measurements existed in the literature for a given pulsar, we extrapolated the flux density at 100 MHz from the 400 MHz flux density in the ATNF catalog using

the measured spectral index if available or −1.6 otherwise. The flux density at the LWA-1 observing frequency was then extrapolated from 100 MHz with a spectral index of 1.4.

Figure 1 shows the difference between low-frequency flux density values extrapolated from 400 MHz and actual low-frequency measurements. This ratio covers two orders of magnitude for pulsars with flux density measurements from the VLSS, and about four orders of magnitude for other pulsars. Clearly, flux density extrapolations for individual pulsars are extremely uncertain. It is hoped that, despite this deficiency in our method, we can draw conclusions that are valid in a statistical sense from our large simulation sample.

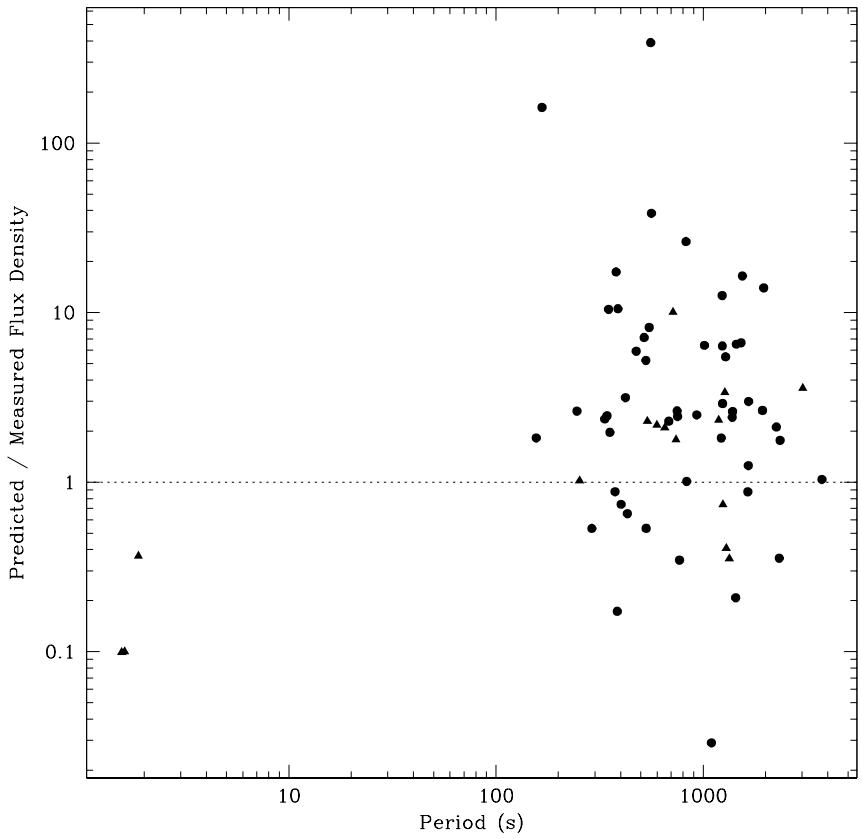

Figure 1 Ratio of predicted to measured low-frequency flux density versus pulse period. Triangles represent pulsars with VLSS flux densities from Cohen et al. (2007), circles are pulsars which only appear in the work of Izvekova et al. (1981). The predicted flux density was extrapolated from the ATNF catalog value at 400 MHz to the frequency of the low-frequency measurement using the method described.

3 Results

Our simulations indicate that a significant number of pulsars will be detectable with LWA-1. Our sample includes 574 pulsars which are in the part of the sky visible to LWA-1

Table 1. Pulsars detectable in 1000 s with LWA-1

Center Frequency (MHz)	Bandwidth (MHz)	Pulsars with S/N $\geq$ 3	Pulsars with S/N $\geq$ 5	Pulsars with S/N $\geq$ 10
72	16	81	57	30
76	8	70	44	27
50	8	29	23	18
24	8	1	1	0

and for which all data necessary for our simulation are available; we estimate that 81 of these are detectable in a relatively short integration time. Table 1 shows the number of pulsars predicted to be detectable in a 1000 s integration with LWA-1 in several observing configurations at 3-, 5-, and 10-σ significance. As expected, pulsars are most easily detectable at the upper end of the LWA band; below the $\sim$ 100 MHz peak of pulsar spectra, all relevant parameters become less favorable to detection as one moves to lower frequency.

Figure 2 shows the 81 pulsars detected at 72 MHz with 16 MHz bandwidth. While most of the detections are long period pulsars, several pulsars with periods shorter than 100 ms are detectable. Figure 3 shows the optimum frequency resolution for each of these detected pulsars. We note that, although we allowed a minimum channel bandwidth of only 0.1 kHz, no detected pulsar had an optimum channel bandwidth less than 0.5 kHz.

4 Conclusions

Our simulations show that several tens of pulsars should be detectable with LWA-1 even with modest integration times. With longer integration times, higher S/N detections will allow novel studies of pulsars at low frequencies.

While this simulation is encouraging and potentially useful in a statistical sense, it is clear that our ability to estimate pulsar flux densities at LWA-1 frequencies is currently limited. As this is the only part of the simulation that is not fairly robust, any improvement in this area would lead to a dramatic improvement in the certainty of predictions such as those presented here.

Conversely, it may not be possible to improve our understanding of low-frequency pulsar spectra without more observational data. The LWA will play an important role here, providing a window on pulsars at low frequencies that have largely been overlooked in the past and expanding our understanding of these enigmatic objects.

References

Cohen, A. S., Lane, W. M., Cotton, W. D., Kassim, N. E., Lazio, T. J. W., Perley, R. A., Condon, J. J., & Erickson, W. C. 2007, AJ, 134, 1245

Cordes, J. M., & Lazio, T. J. W. 2002, astro-ph/0207156

Haslam, C. G. T., Stoffel, H., Salter, C. J., & Wilson, W. E. 1982, A&AS, 47, 1

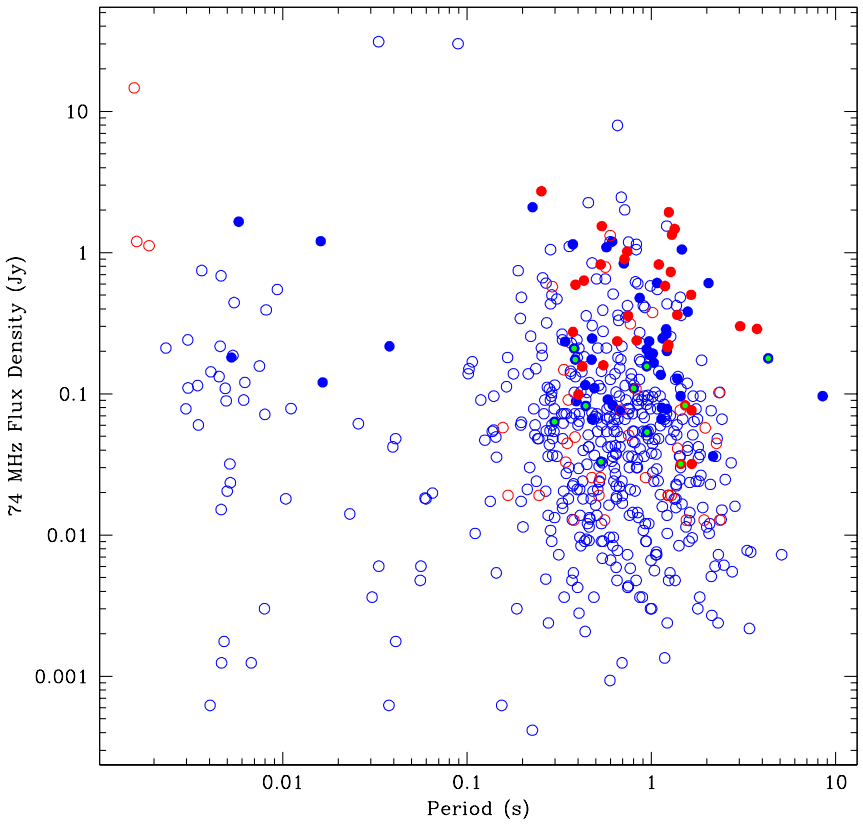

Figure 2 Simulated pulsar detections in flux density and pulse period. 74 MHz flux density is plotted versus pulse period for the sample of 574 pulsars available to LWA-1. Open circles represent pulsars not detected in our simulation, while filled circles are detections of at least $3\,\sigma$ in 1000 s at 72 MHz with 16 MHz of bandwidth. Filled points with green dots would not have been detected at 76 MHz with 8 MHz bandwidth. Red points are pulsars with published low-frequency flux density measurements, while blue points are pulsars whose 74 MHz flux has been extrapolated from measurements at 400 MHz.

Izvekova, V. A., Kuzmin, A. D., Malofeev, V. M., & Shitov, I. P. 1981, Ap&SS, 78, 45

Kraus, J. D. 1988, Antennas (Boston: McGraw-Hill)

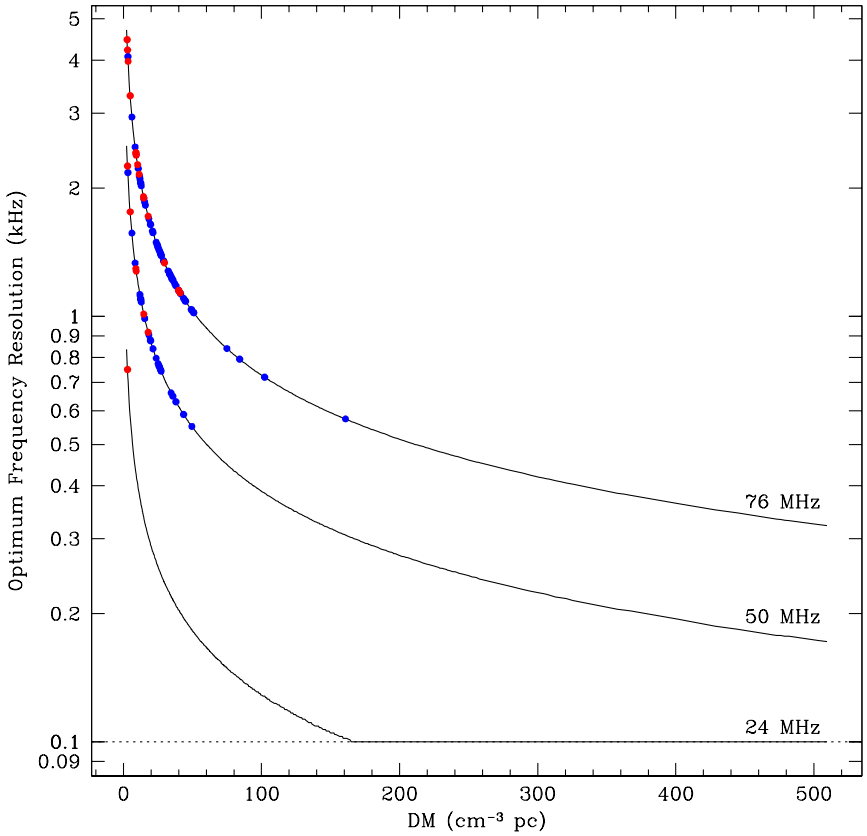

Figure 3 Optimum frequency resolution as a function of DM at three frequencies spanning the LWA-1 frequency range. Points represent pulsars detected in the simulation with 8 MHz bandwidth at three different center frequencies. Red points are pulsars with published low-frequency flux density measurements, while blue points are pulsars whose low-frequency flux density has been extrapolated from measurements at 400 MHz.